JOURNAL OF MATERIALS SCIENCE **34** (1999) 3035–3041

Reaction characteristics of $La_{0.84}Sr_{0.16}CrO_3$ formation

A. L. WAGNER*, A. J. JACOBSON‡, J. T. RICHARDSON*, D. LUSS*§
*Departments of *Chemical Engineering and ‡Chemistry, University of Houston,*
Houston TX 77204-4792, USA
E-mail: dluss@uh.edu

We studied the kinetics of $La_{0.84}Sr_{0.16}CrO_3$ formation from a precursor consisting of La and Sr chromium oxides and carbonates made by spray roasting. Pure $LaCrO_3$ becomes cubic at temperatures exceeding 1900 °C. Strontium doping lowers the transition temperature, for example, that of $La_{0.84}Sr_{0.16}CrO_3$ is 1700 °C. This transition is gradual and occurs over a 700 °C range upon heating and cooling. Low temperature (LT) air calcination (450 °C) of the precursor yields a mixture of $LaCrO_4$ and $SrCrO_4$, which following 20 h of heating at 1440 °C produces a homogeneous powder. Secondary electron images of this precursor reveal dense spheres with 95% of the theoretical density of $La_{0.84}Sr_{0.16}CrO_3$. High temperature (HT) calcination (800 °C) yields a mixture of $LaCrO_3$ and $SrCrO_4$, which following 40 h of heating at 1500 °C produces a uniform product. The LT and HT calcination causes oxygen loss.

1. Introduction

Interconnects in solid oxide fuel cells (SOFC) must be stable in both oxidizing and reducing environments at the operating temperature of 1000 °C. The Sr doped perovskite oxide $LaCrO_3$ is a candidate interconnect material since it exhibits high electronic conductivity, low ionic conductivity, phase-stability under SOFC operating conditions, a thermal expansion coefficient that matches other SOFC components and is chemically compatible with YSZ (electrolyte), $La_{1-x}Sr_xMnO_3$ (cathode), and nickel zirconia cermet (anode) [1].

At room temperature, pure $LaCrO_3$ has a slightly distorted perovskite unit cell. A symmetry change from orthorhombic to rhombohedral occurs above 560 K [2, 3]. Lanthanum chromite forms a single phase when doped with strontium mole fractions of up to 0.35. The volume of the $LaCrO_3$ orthorhombic unit cell is 233.9 $Å^3$ ($a = 5.512$ Å, $b = 7.752$ Å, $c = 5.476$ Å) [4]. The unit cell volume of $LaCrO_3$ slightly decreases with increasing dopant concentrations, and the X-ray diffraction patterns of the doped and undoped $LaCrO_3$ are very similar. $La_{0.84}Sr_{0.16}CrO_3$ has the most favorable properties for a fuel cell interconnect [5] and its orthorhombic to rhombohedral transition temperature is ∼160 K. Pure $LaCrO_3$ becomes cubic at temperatures exceeding 1900 K [6]. The addition of Sr (up to 0.35 mol. fraction) lowers the rhombohedral to cubic transition temperature by at least 200 K. We studied this phase change for both doped and undoped $LaCrO_3$.

The decrease in unit cell volume during the transformation of an amorphous mixture of La and Sr chromium oxides and carbonates into $La_{0.84}Sr_{0.16}CrO_3$ may be followed *in situ* by high temperature powder X-ray diffraction (HT-XRD). The transformation from amorphous ash (the product of the spray roasting procedure) to pure homogeneous $La_{0.84}Sr_{0.16}CrO_3$ is not well understood. Bates *et al.* [7] have proposed a mechanism by which strontium chromate melts and then diffuses throughout the $LaCrO_3$ structure. This mechanism assumes that the starting material contains $LaCrO_3$, along with some Sr phases such as $SrCrO_4$, but does not explain the inhomogeneous product that forms when the precursor is heated below 1500 °C.

Large-scale production of LSC begins with the synthesis of an amorphous precursor, which is calcined at an intermediate temperature, pressed into pellets and then reacted at a high temperature. It is desirable to conduct the reaction in air, while optimizing the reaction time and temperature to minimize the production cost. Co-sintering of the components of tubular SOFCs after plasma spraying is commonly used for this purpose. Co-sintering requires that the interconnect material attain high density, while the highly porous manganite air-electrode remains stable. LSC is non-porous if it sinters to 95% or greater of the theoretical (full) density [8].

The purpose of this study is to determine the most favorable reaction conditions and procedure for large scale production of Sr doped $LaCrO_3$ powder for fuel cell interconnects. We used high temperature X-ray diffraction (HT-XRD), thermogravimetric (TG) and differential thermal analysis (DTA) and electron microprobe analysis to study the reaction mechanism and

---

§ Author to whom all correspondence should be addressed.

kinetics of $La_{0.84}Sr_{0.16}CrO_3$ and the effect of gas environment on the reaction rate.

2. Experimental

2.1. Powder synthesis and stoichiometry

Precursor powders with the overall composition of $La_{0.84}Sr_{0.16}CrO_{3-\delta}$ were manufactured by Praxair. In that process, La, Sr, and Cr oxides are intimately mixed and spray roasted in the presence of an organic solid. The powders are of high purity and have a very narrow particle size distribution with an average size of ~2 μm. Inductively coupled plasma spectroscopy was used to verify the $La_{0.84}Sr_{0.16}CrO_3$ stoichiometry. The precursor powder contained 3.8 wt % carbon (measured with a LECO WR-112 wide range carbon determinator). The loose powder was calcined in a bench top furnace in air.

2.2. Equipment and sample preparation

Differential thermal analysis (DTA) and thermogravimetric analysis (TGA) were conducted with a Seiko TG/DTA 320, using loose powder held in a Pt weighing pan and alumina as a reference. The gas environment was controlled by Tylan N_2 and O_2 mass flow controllers with an overall flow rate of 200 sccm.

X-ray diffraction patterns were measured with a Siemens D5000 powder diffractometer fitted with a Buehler HDK 3.1 hot stage, capable of operating at temperatures up to 1300 °C in an oxidizing environment and a Braun position sensitive detector. The temperature was controlled by a Buehler LET 2401 unit utilizing a 90%Pt/10%Rh strip (Johnson-Matthey) sample holder and heating element. A thin reactant film (thickness of about 30–80 μm) was deposited on the Pt/Rh strip by air-brushing a slurry of the powder in absolute ethanol. The sample thickness was adjusted so that the product of μ (the linear absorption coefficient), and τ (the sample thickness) ranged between 0.5 and 0.8. A 90%Pt/10%Rh environmental circular heater surrounded the sample with a 30° arc at the top removed to allow for the passage of X-rays.

An electron microprobe (JXA-8600 JEOL Superprobe) was used to produce backscattered electron images (BEI) and secondary electron images (SEI) and to perform wavelength dispersive spectrometry (WDS). The WDS provided an elemental analysis of a one square micron section of the sample. Energy dispersive spectroscopy (EDS) was performed in the microprobe to detect impurities and provide a qualitative measure of homogeneity on the micron scale. Sample preparation for microprobe measurements consisted of binding the powders in epoxy, polishing the surface, and carbon coating before measurements were taken.

Loose LSC powders were pressed into pellets uniaxially at room temperature by a pressure of 10,000 PSI. The true volume of the loose powder and pressed pellets (as a measure of porosity) were determined with a helium pycnometer (Quantachrome).

3. Results and discussion

3.1. Characterization of the precursor and the reaction product

X-ray diffraction analysis showed that the precursor is an amorphous mixture of oxides and carbonates with small amounts of $LaCrO_4$ (<10%) and $LaCrO_3$ (<10%) present. Air calcination removes the residual carbon, and $La_{0.84}Sr_{0.16}CrO_3$ is formed by heating the calcined precursor to a high temperature. Most studies of LSC crystal structure, sintering, and electrical conductivity have used samples prepared by heating the precursor at 1500–1700 °C in an inert (low pO_2) atmosphere for over 5 hours and using X-ray diffraction to test the homogeneity [9–11]. However, XRD patterns of non-homogeneous and homogeneous LSC samples are virtually identical at room temperature. Only at high temperatures (about 1100 °C) is it possible to discern inhomogeneities with XRD using the high resolution position sensitive detector operating in fixed mode.

We used XRD to determine the effect of heat treatment on the precursor ash. Fig. 1 compares the patterns

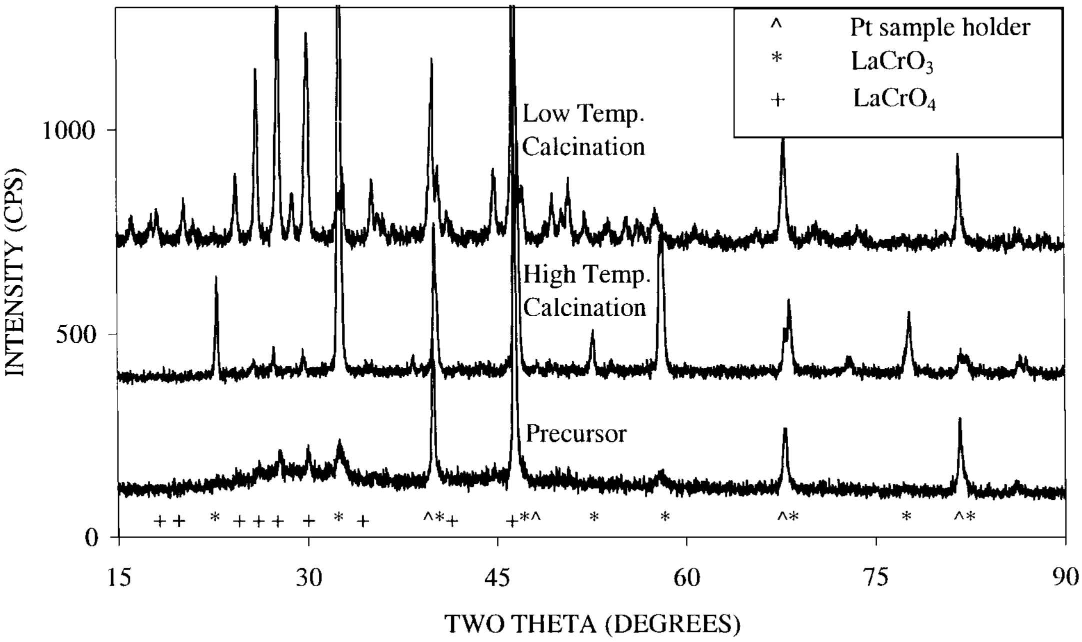

Figure 1 X-ray diffraction patterns of the $La_{0.84}Sr_{0.16}CrO_3$ precursor: raw precursor, after low temperature calcination (450 °C), and after high temperature calcination (800 °C).

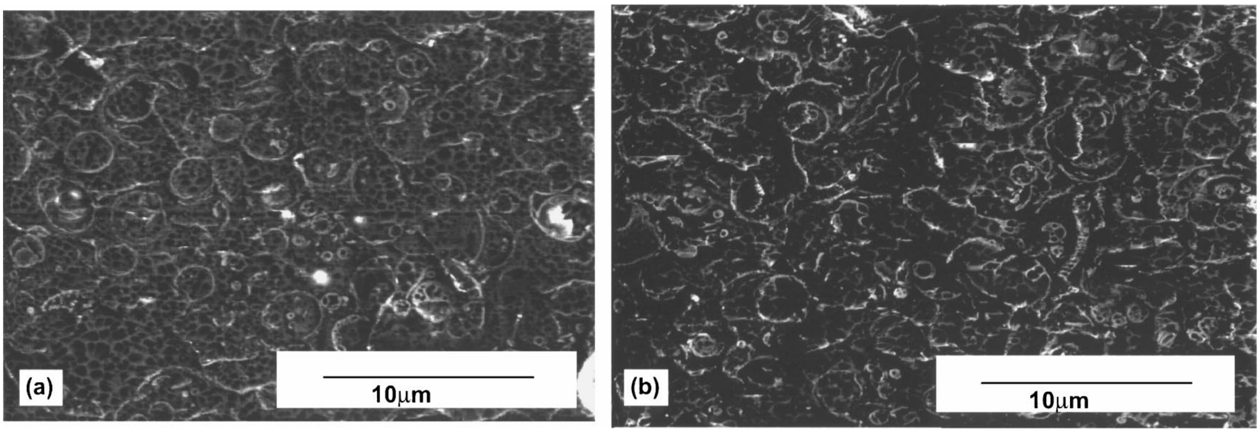

Figure 2 Secondary electron images of the precursor after (a) low temperature calcination (450 °C) and (b) high temperature calcination (800 °C).

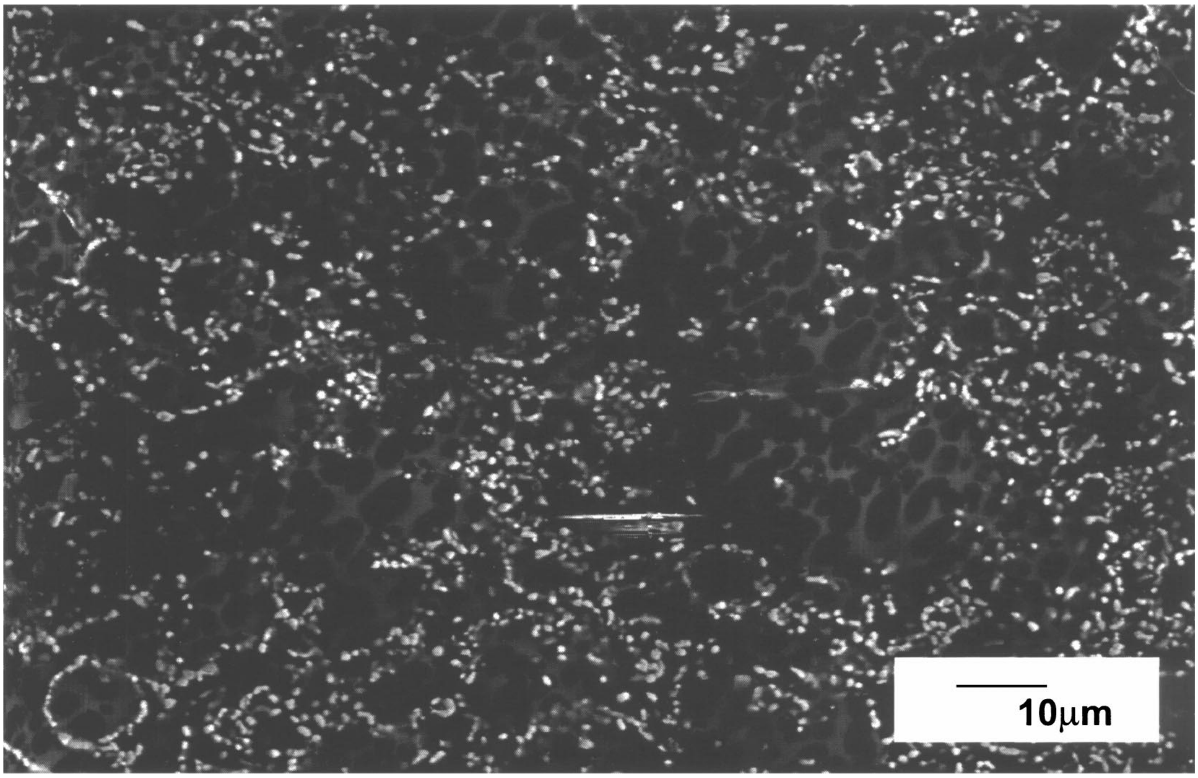

Figure 3 Secondary electron image of the resulting $La_{1-x}Sr_xCrO_3$ mixture after heating the HT calcined precursor to 1250 °C for 20 h in air.

of the raw precursor, a sample heated in air at 800 °C for 2 h (high temperature calcination), and a sample heated in air at 450 °C for 50 h (low temperature calcination). The JCPDS files indicate that the high temperature calcined sample (HT) consists mainly of $La(Sr)CrO_3$ and a small amount of $La(Sr)CrO_4$. The low temperature calcined sample (LT) contained only the $La(Sr)CrO_4$ phase. Secondary electron images (SEI) (Fig. 2) show that these compounds (the LT and HT) comprise primarily a single phase that appears lighter in intensity than the dark background of void space. The powders are porous and consist of hollow spheres that are probably composed of small individual particles connected at the grain boundaries [12]. Lanthanum-rich phases are indicated by brighter regions in the SEI. Wavelength dispersive spectrometry (WDS) reveals that these materials are homogeneous within the resolution of the beam (5–10 μm^3).

The diffraction patterns indicate that upon heating to 1150 °C in air, the material becomes a single phase as all the $SrCrO_4$ peaks disappear. The characteristic reflections of $LaCrO_3$ are shifted by 0.02° to 0.04° to higher values of 2θ. A single phase diffraction pattern is usually assumed to prove complete incorporation of Sr into the $LaCrO_3$. However, $SrCrO_4$ peaks disappear almost immediately at temperatures exceeding 1250 °C, indicating melting of the Sr-rich phase. Sr-rich and La-rich phases were detected by the WDS of samples heated to 1250 °C and then slowly cooled to room temperature. Fig. 3 is a secondary electron image of this sample. Wavelength dispersive spectrometry shows that the HT calcined precursor sample of $La_{1-x}Sr_xCrO_3$ with x varying spatially between 0.00 to 0.36 and the overall stoichiometry (0.84 : 0.16 : 1 : 3) becomes homogeneous following 40 h heating at 1500 °C in air. X-ray diffraction patterns of a LT calcined precursor

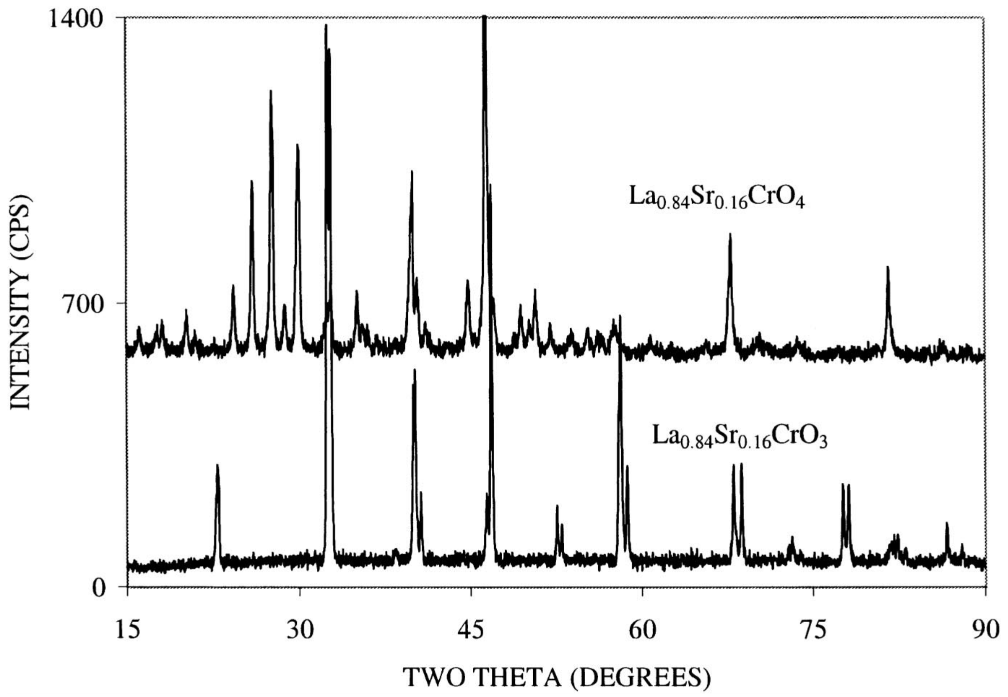

Figure 4 XRD patterns of a LT calcined precursor (top) and a LT calcined precursor heated to 1440 °C for 20 h (bottom).

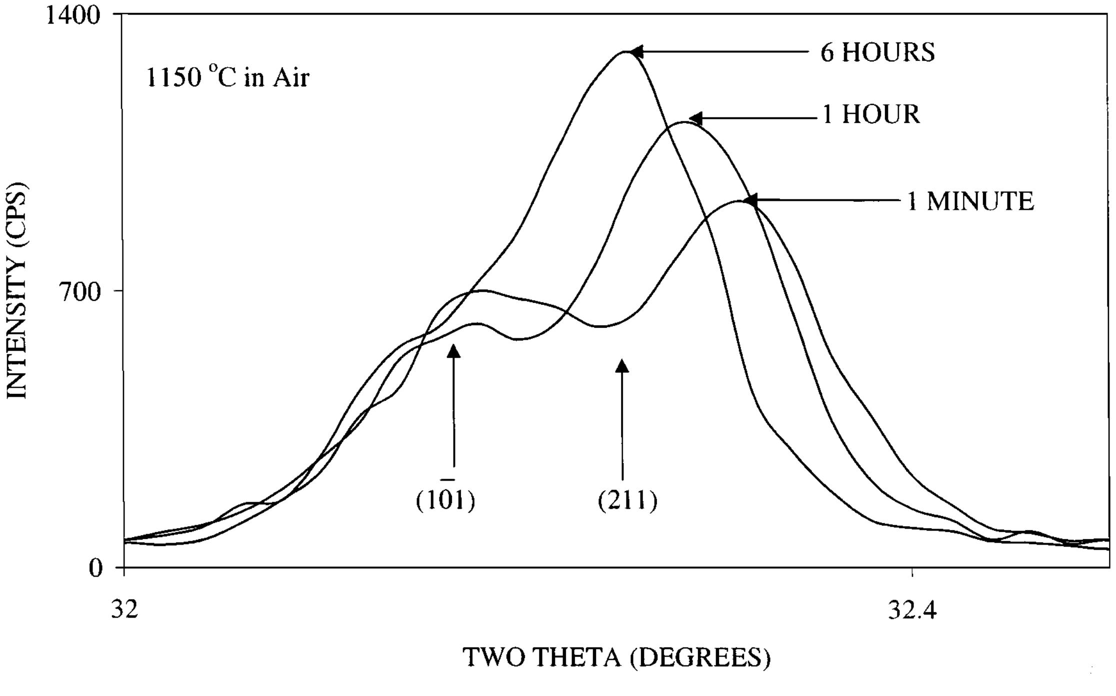

Figure 5 The most intense peak of $LaCrO_3$ XRD patterns taken after 1 min, 1 h, and 6 h at 1150 °C.

(Fig. 4) show that a single rhombohedral phase exists at room temperature following heating to 1440 °C. This observation agrees with all previous studies of $La_{0.84}Sr_{0.16}CrO_3$.

3.2. Characterization of the phase transition

High temperature XRD was used to follow the progress of doping Sr into $LaCrO_3$. The temporal variations of the strongest reflections of the single phase upon heating for several hours at 1150 °C are shown in Fig. 5. The $(1\,0\,\bar{1})$ and $(2\,1\,1)$ reflections of rhombohedral $LaCrO_3$ converge, and shift to higher and lower 2θ positions respectively. The rhombohedral to cubic phase transition temperature decreased as Sr incorporated into the $LaCrO_3$ from the reported ~1900 to ~1700 C. Formation of the cubic phase is evidenced by the growth of a single reflection from the two rhombohedral reflections.

The rhombohedral to cubic phase transition of pure $LaCrO_3$ has been reported between 1030 °C [13] to 1650 °C [14]. We found it to occur between 1100 and 1900 °C. Doped $LaCrO_3$ with 0.16 mol fraction of Sr decreases this transition temperature range to between 1000 and 1700 °C. Unlike the sharp orthorhombic to rhombohedral transition at 270 °C, the transition

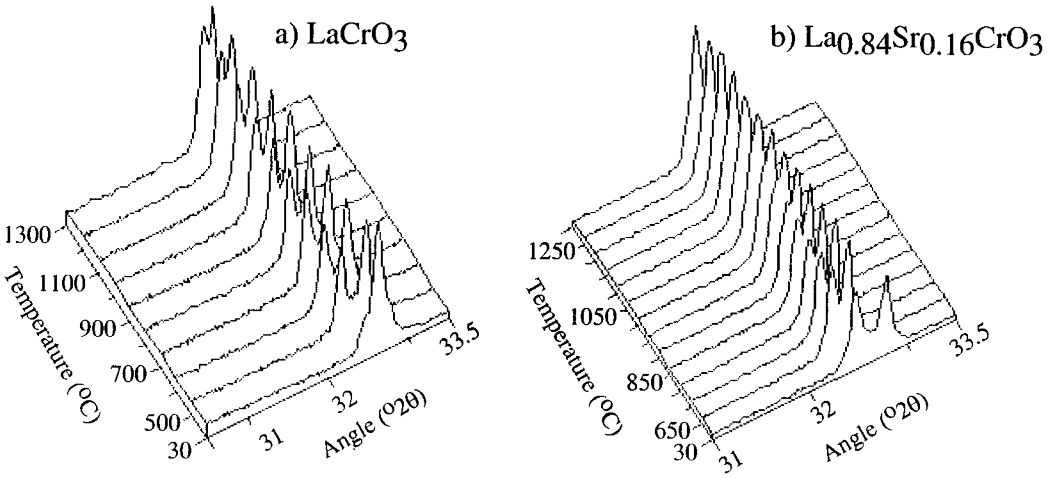

Figure 6 The most intense peak of XRD patterns of (a) $LaCrO_3$ and (b) $La_{0.84}Sr_{0.16}CrO_3$ taken at increasing temperatures.

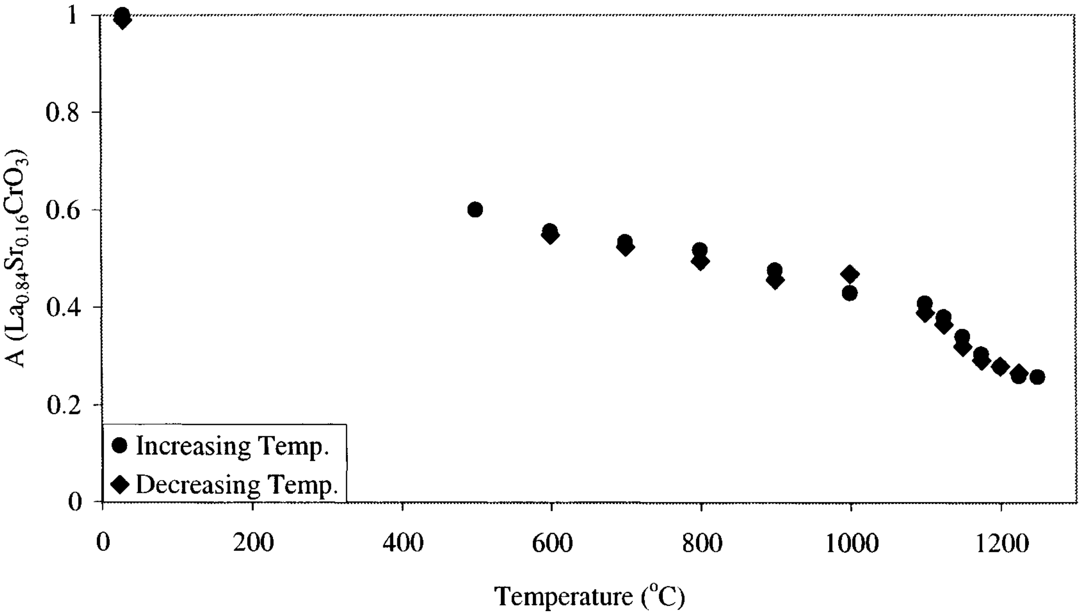

Figure 7 Plot of the normalized rhombohedral angle α as a function of temperature upon heating and cooling of $La_{0.84}Sr_{0.16}CrO_3$.

to the cubic phase is gradual with increasing temperature. Fig. 6 shows the rhombohedral reflections as a function of temperature for both pure $LaCrO_3$ and $La_{0.84}Sr_{0.16}CrO_3$. The phase transition is not sharp and cannot be said to occur at a specific temperature. Fig. 7 is a plot of A, the normalized rhombohedral angle α, defined as

$$A_T = \frac{\alpha_{30\,^\circ\mathrm{C}} - \alpha_T}{\alpha_{30\,^\circ\mathrm{C}} - 60^\circ}, \tag{1}$$

where T is a given temperature and α is calculated from the 2θ positions of the $(1\,0\,\bar{1})$ and $(2\,1\,1)$ rhombohedral reflections. The plot shows that for $La_{0.84}Sr_{0.16}CrO_3$, A_T is independent of whether the powder is heated or cooled. The lattice constants of this distorted cubic phase depend on the temperature but not on the temperature history, as indicated by lack of hysteresis upon cooling the sample. An unexpected inflection point at ~1100 °C is also seen from this plot. By extrapolation, the sample should become cubic at ~1700 °C. Fig. 8 indicates some hysteresis when $LaCrO_3$ is heated above 1200 °C and then cooled.

3.3. Reaction mechanism

The precursor ash contains 3.8 wt% carbon. The $La(Sr)CrO_4$ sample carbon content is 0.24 wt% and that of $LaCrO_3/SrCrO_4$ is 0.05 wt%. Thermogravimetric measurements show that $La(Sr)CrO_4$ heated in air looses weight as it forms $La(Sr)CrO_3$, due to loss of oxygen and residual carbon upon heating. As $LaCrO_3/SrCrO_4$ transforms into $La(Sr)CrO_3$, the oxygen and residual carbon weight loss is exceeded by 4.3% of that predicted by the reaction mechanism proposed below. This difference may be attributed to water absorbed by the powder from the atmosphere. When heated in pure N_2, carbon is not removed and the oxygen weight loss is exceeded by 5% of the predicted value. These results agree with HT-XRD patterns which indicate that the overall low temperature reaction is

$$(1-x)\,LaCrO_4 + x SrCrO_4 \rightarrow La_{1-x}Sr_xCrO_3 + 0.5O_2 \tag{2}$$

while the high temperature reaction is

$$(1-x)\,LaCrO_3 + x SrCrO_4 \rightarrow La_{1-x}Sr_xCrO_3 + \frac{x}{2}O_2 \tag{3}$$

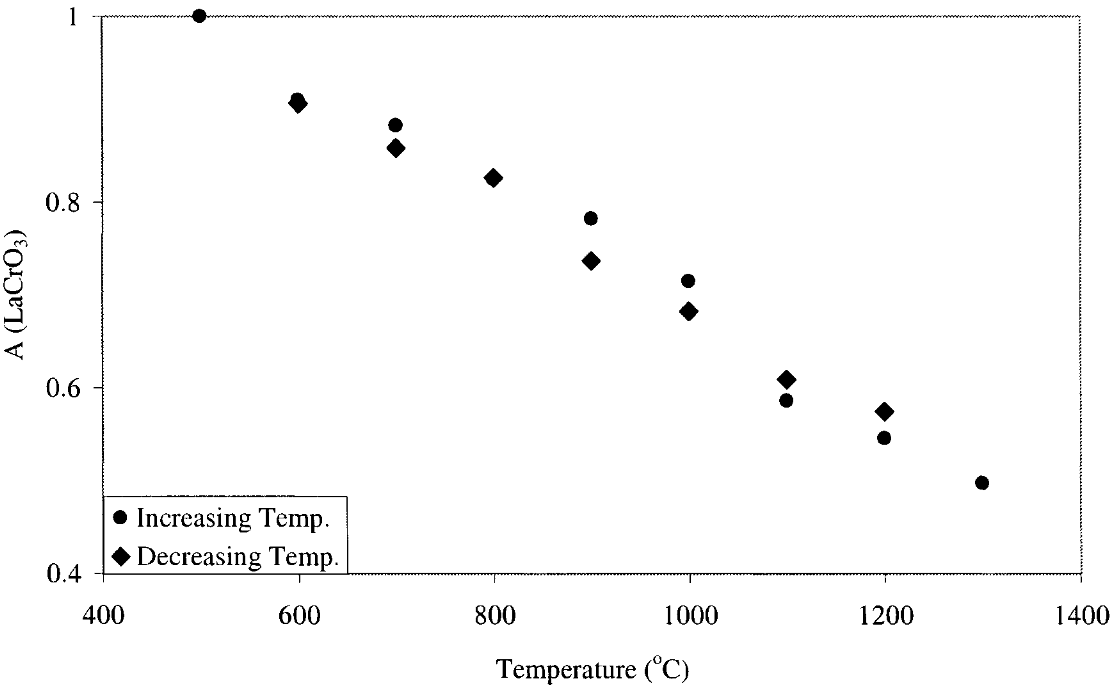

Figure 8 Plot of the normalized rhombohedral angle α as a function of temperature upon heating and cooling of $LaCrO_3$.

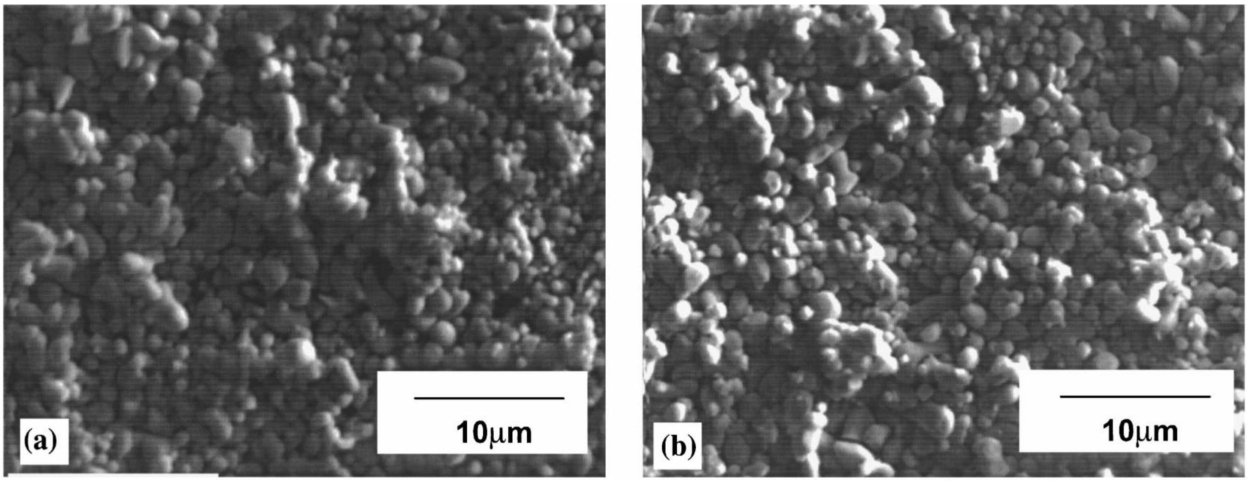

Figure 9 Secondary electron images of $La_{1-x}Sr_xCrO_3$ after heating of the LT calcined precursor at 1250 and 1440 °C for 40 hrs.

The value of x in the product varies spatially in the range of (0.07, 0.32), with the volume average being equal to the initial value. This indicates that chromium oxides do not vaporize below 1300 °C.

3.4. Electron probe micro-analysis

Thermogravimetric analysis and HT-XRD are not sufficient to determine the homogeneity of the product. Obtaining homogeneous products free of local concentration variations requires extensive heating at temperatures exceeding 1500 °C. While no oxygen is liberated from these samples and their room temperature diffraction patterns exhibit only rhombohedral reflections associated with the doped species, uniform doping of Sr onto 16% of the perovskite A lattice sites may not be realized. WDS indicates that local concentration gradients exist even in samples heated for 20 h at 1500 °C. Comparison of the secondary electron images (SEI) of products obtained by moderate (1250 °C) and high (1440 °C) temperature heating cycles (Fig. 9) with those in Fig. 2 shows that the regions of high La or Sr concentration shrink as the calcination temperature increases. Moreover, SEI indicates that the ring structure fragments into smaller bright regions, indicating a decrease in the size of the crystallites. This transformation decreases the porosity and increases the density of the sintered powder. Fragmentation of the larger particles is seen in Fig. 2. No local nonuniformities (down to the width of the electron beam, 1 μm) were detected in a sample exposed to high temperature for 40 h. Wavelength dispersive spectrometry is the only conclusive proof that full incorporation of Sr into $LaCrO_3$ has been accomplished.

3.5. Density measurements

Rietveld refinement [15] of the full diffraction pattern of the fully incorporated $La_{0.84}Sr_{0.16}CrO_3$ was conducted

TABLE I Percentage of theoretical density (6.593 g/cm^3)

Material	Powder	Pellet
Precursor	64.3	70.5
HT calcined precursor	72.2	75.6
LT calcined precursor	48.9	53.6
1500 °C for 40 h (HT)	95.3	96.2
1440 °C for 20 h (LT)	95.2	95.8

using GSAS© software. The lattice constant was determined to be 3.874 Å, yielding a unit cell volume of 58.14 Å^3 and a theoretical density of 6.593 g/cm^3. The true powder density and percentage deviation from the theoretical density are reported as a function of the temperature in Table I. These results indicate that a product with >95% of the theoretical density may be produced by a heat treatment and sintering of the LT calcined precursor at a temperature of 1440 °C.

4. Conclusions

Low temperature ($T < 500$ °C) calcination of a precursor ash yields a mixture of $LaCrO_4$ and $SrCrO_4$. It can be transformed to a uniform product, that can be sintered to a density exceeding 95% of the theoretical value, by 20 h of heating at 1440 °C. Higher calcination temperatures (800 °C) yield a mixture of $LaCrO_3$ and $SrCrO_4$. It can be transformed to a uniform $La_{0.84}Sr_{0.16}CrO_3$ by 40 h of heating at a temperature exceeding 1500 °C.

The presence of Sr in the $LaCrO_3$ matrix decreases the complete rhombohedral to cubic phase transition temperature from 1900 to 1700 °C. A gradual phase transition to a distorted cubic perovskite structure occurs between 1000 °C and the complete phase transition temperature of 1700 °C.

Electron microprobe analysis is a reliable check if the system is uniformly doped and homogeneous at the micron level. Spatial nonuniform doping is not detected by XRD or TGA. Thus, previous claims about homogeneity of the doped material may have to be re-examined.

Acknowledgements

The authors are thankful to the Materials Research Science and Engineering Center at the University of Houston (MRSEC-UH) and the Texas Center for Superconductivity at the University of Houston (TcSUH) for sponsoring this research. Electron microprobe analysis was performed by Dr. Kent Ross of TcSUH. The authors would also like to thank Dr. Visiliki Milonopoulou and Dr. Ken Forster for valuable suggestions and insight.

References

1. S. C. SINGHAL, in Proceedings of the International Forum on Fine Ceramics (Japan Fine Ceramics Center, Nagoya, Japan, 1992) pp. 159–167.
2. J. S. RUIZ, A. M. ANTHONY and M. FOEX, *C. R. Acad. Sc. Paris Ser. B* **264** (1967) 1271.
3. S. SRILOMSAK, D. P. SCHILLING and H. U. ANDERSON, in "Proc. of the 1st Int. Symp. on Solid Oxide Fuel Cells," edited by S. C. Singhal (The Electrochemical Society, Pennington, NJ, 1989) pp. 129–140.
4. T. R. ARMSTRONG, J. W. STEVENSON, L. R. PEDERSON and P. E. RANEY, *J. Electrochem. Soc.* **143** (1996) 2919.
5. T. G. NAKAMURA and L. J. GAUCKLER, *Mater. Res. Bull.* **14** (1979) 679.
6. J.-P. TRAVERSE and R. BERJOAN, *C. R. Acad. Sc. Paris Ser. C* **276** (1973) 1167.
7. J. L. BATES, T. R. ARMSTRONG, L. A. CHICK, W. J. WEBER, C. A. WINDISCH and G. E. YOUNGBLOOD, in "Alternative Electrodes and Interconnections for Solid Oxide Fuel Cells" (Pacific Northwest Laboratories, Richland, WA 1993) p. 22.
8. J. L. BATES, in "Energy Progress and Environmental Protection," Energy Technology XVI, 1989, p. 205.
9. C. P. KHATTAK and D. E. COX, *Mater. Res. Bull.* **12** (1977) 463.
10. L. GROUPP and H. U. ANDERSON, *J. Amer. Ceram. Soc.* **59** (1976) 449.
11. N. SAKAI, T. KAWADA, H. YOKOKAWA, M. DOKIYA and I. KOJIMA, *ibid.* **76** (1993) 609.
12. J. L. BATES, T. R. ARMSTRONG, L. A. CHICK, W. J. WEBER, C. A. WINDISCH and G. E. YOUNGBLOOD, in "Alternative Electrodes and Interconnections for Solid Oxide Fuel Cells" (Pacific Northwest Laboratories, Richland, WA 1993) p. 14.
13. J. S. RUIZ, A. M. ANTHONY and M. FOEX, *C. R. Acad. Sc. Paris Ser. B* **264** (1967) 1271.
14. S. GELLER and P. M. RACCAH, *Physical Review B* **2(4)** (1970) 1167.
15. H. M. RIETVELD, *J. Appl. Cryst.* **2** (1969) 65.

Received 2 November 1998
and accepted 13 January 1999